

**SUPPORTING INFORMATION**

**FOR**

**Pseudoaromaticity-Driven, Transition Metal Detection by  
Squaraine-Derived Enol Phosponium Ylide Chemodosimeters**

Raïssa Twiringiyimana and Brandon L. Ashfeld\*

*Department of Chemistry and Biochemistry, University of Notre Dame, Notre Dame, Indiana 46556*

*Corresponding Author Email: [bashfeld@nd.edu](mailto:bashfeld@nd.edu)*

**Contents**

General	S2
Experimental Procedures	S2
Beer's law analysis & Titration graphs	S3-S123
NMR Spectra	S14-S19
References	S20

## I. GENERAL

Solvents and reagents were reagent grade and used without purification unless otherwise noted. All reactions were carried out in flame dried glassware unless otherwise specified. Squaraine dyes **4** and ylides **3** were prepared according to literature procedures.<sup>1</sup> <sup>1</sup>H nuclear magnetic resonance (NMR) spectra were obtained at either 400 or 500 MHz. <sup>13</sup>C NMR were obtained at 100 or 125 MHz. Chemical shifts are reported in parts per million (ppm,  $\delta$ ), and referenced from the TMS. Coupling constants are reported in Hertz (Hz). Spectral splitting patterns are designated as s, singlet; d, doublet; t, triplet; q, quartet; m, multiplet; comp, complex; app, apparent; and br, broad. High- and low-resolution fast atom bombardment (FAB) measurements were made with a Bruker MicroTOF II mass 207 spectrometer. Absorption spectra were collected using V-670 JASCO UV-Vis spectrophotometer. Fluorescence spectra were collected using a Horiba Fluoromax-4 Fluorometer with FluoroEssence software. Analytical thin layer chromatography (TLC) was performed using EMD 250 micron 60 F254 silica gel plates, visualized with UV light (250 nm lamp) and stained with either *p*-anisaldehyde, ceric ammonium nitrate or potassium permanganate solutions. Flash column chromatography was performed according to Still's procedure (Still, W. C.; Kahn, M.; Mitra, A. *J. Org. Chem.* **1978**, *43*, 2923) using Silicycle SiliaFlash P60 40-63  $\mu$ m 60 Å silica gel.

## II. EXPERIMENTAL PROCEDURES

**<sup>1</sup>H NMR spectroscopy Experiments:** A solution of ylide **3**<sup>1</sup> (0.4 mL, 0.02 M) in CDCl<sub>3</sub> was added to a solution of ML<sub>n</sub> (0.4 mL, 0.02 M). <sup>1</sup>H NMR (500 MHz) was used to monitor the metal-mediated conversion of ylide **3** to squaraine **4** at rt, revealing complete conversion with [Rh(COD)Cl]<sub>2</sub>, [Ir(COD)Cl]<sub>2</sub>, and Pd(OAc)<sub>2</sub>, and partial conversion with Au(PPh<sub>3</sub>)Cl and Rh(PPh<sub>3</sub>)<sub>3</sub>Cl. Integration of hydroxy group peaks determined the **4/3** ratio.

**Concentration experiment of ylide **3a**:** Separately, solutions of **3a** (100 mM, 50 mM, 10 mM, 5 mM, 1 mM, 500  $\mu$ M and 100  $\mu$ M) were prepared in CDCl<sub>3</sub>, and to monitor the effect of concentration on ylide **3a**, the samples were analyzed by <sup>1</sup>H NMR spectroscopy. The ratio of **3a/4a** was determined by <sup>1</sup>H NMR integration of hydroxy group peaks.

**General procedure: Titrations monitored by UV-Vis spectroscopy:** Separately, stock solutions of **3** (5 $\mu$ M in DMSO) and ML<sub>n</sub> (50 $\mu$ M in DMSO) were prepared. A 1 ml aliquot of the stock solution containing solution **3** was placed in a 10.00 mm helma<sup>TM</sup> quartz, silica and glass standard cuvette, and the initial absorbance was measured at the indicated wavelength. A 10  $\mu$ L aliquot (0.1 eq.) of the requisite transition metal complex in DMSO was added to the cuvette containing solution **3** and mixed for 5 min to ensure equilibration. The absorbance was measured again, and the process was repeated until a total of 1.5 equivalents of the metal had been added to the phosphonium ylides solution.<sup>2</sup>

**General procedure: Fluorescence titrations of metals with oxindole ylide **3b**:** Separately, stock solutions of **3** (5 $\mu$ M in DMSO) and ML<sub>n</sub> (i.e., Pd(OAc)<sub>2</sub> and HgCl<sub>2</sub>) (50 $\mu$ M in DMSO) were prepared. A 1 mL aliquot of oxindole ylide **3b** solution was transferred to the fluorescence cuvette and initial fluorescence was measured. Titration was performed by adding successive 10  $\mu$ L of the ML<sub>n</sub> to the oxindole ylide **3b** solution and spectra were recorded 5 min after each aliquot addition.

### Beer's law analysis of SQ 4a in DMSO

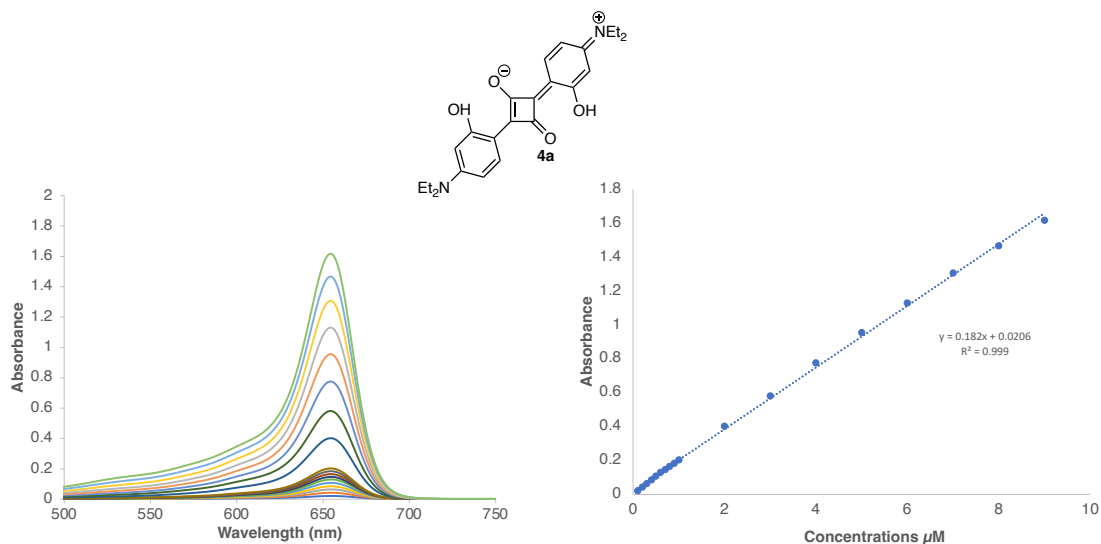


**Figure S1:** Beer's law analysis of squaraine of **SQ 4a** from 0.1 µM to 9 µM. Linearity is maintained as high as 1.61 absorbance units at 655 nm and an extinction coefficient of  $1.82 \times 10^7$  L mol<sup>-1</sup>cm<sup>-1</sup> was obtained.

UV-Vis spectral analysis of **4a** in DMSO is shown in **Figure S1**. Beer's law analysis shows a  $\lambda_{\text{max}}$  at 655 nm over the concentration range tested. Linear adherence to the Beer plot was maintained as high as 1.61 absorbance units. The molar extinction coefficient in DMSO was determined to be  $1.82 \times 10^7$  L mol<sup>-1</sup> cm<sup>-1</sup> from the slope of the absorbance/concentration plot at 655 nm for **4a**.

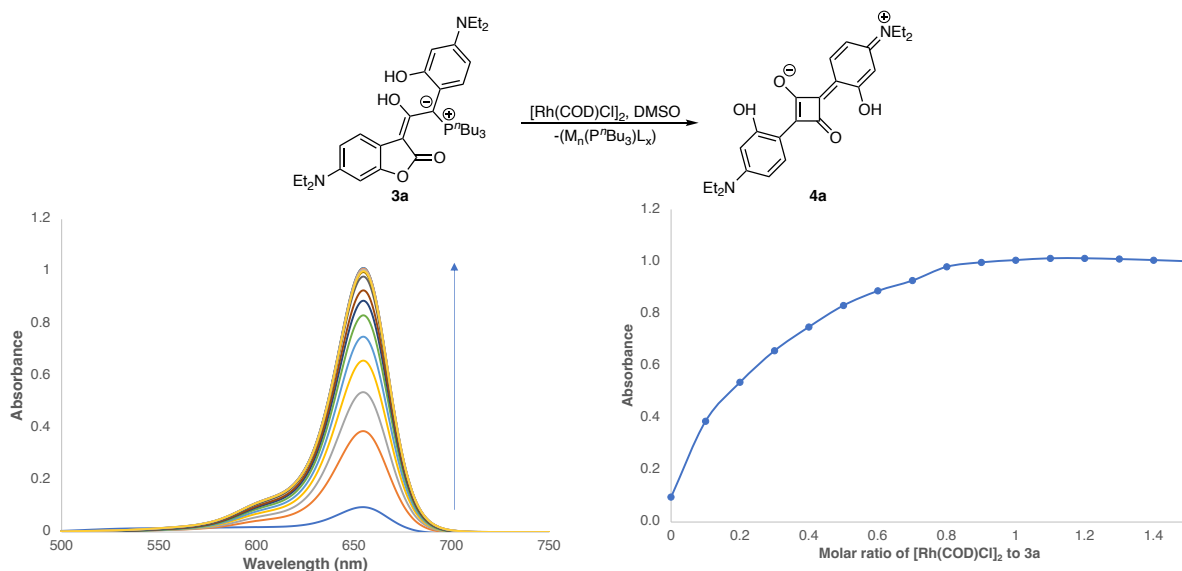


**Figure S2:** Titration of [Rh(COD)Cl]<sub>2</sub> into a solution of benzofuranone ylide **3a** at 5.46 µM in DMSO.

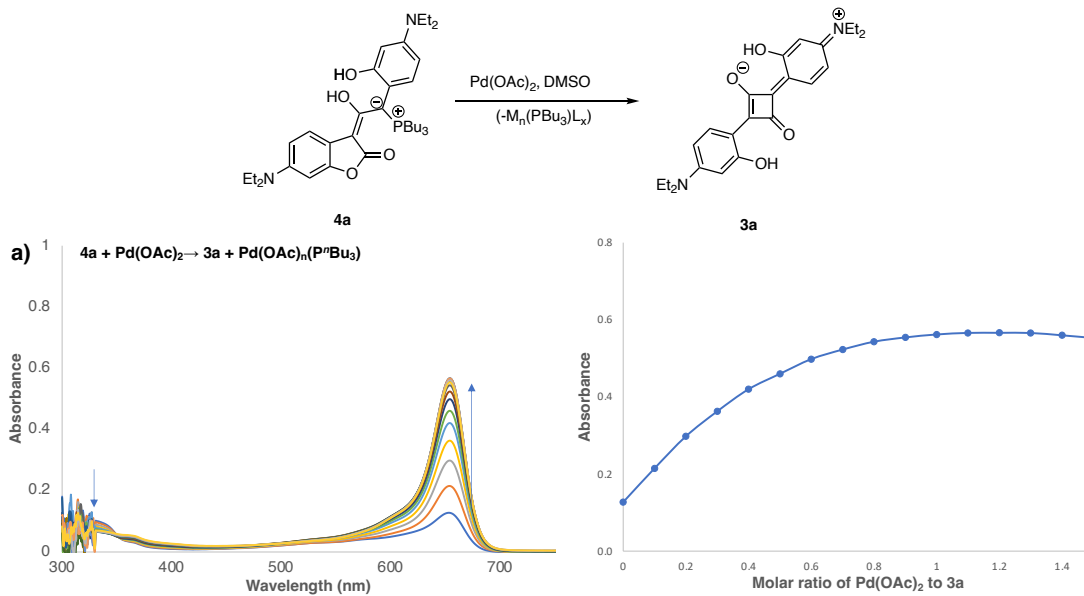


**Figure S3:** Titration of 50.3  $\mu$ M of  $Pd(OAc)_2$  into a solution of benzofuran ylide **4a** at 4.97  $\mu$ M in DMSO.

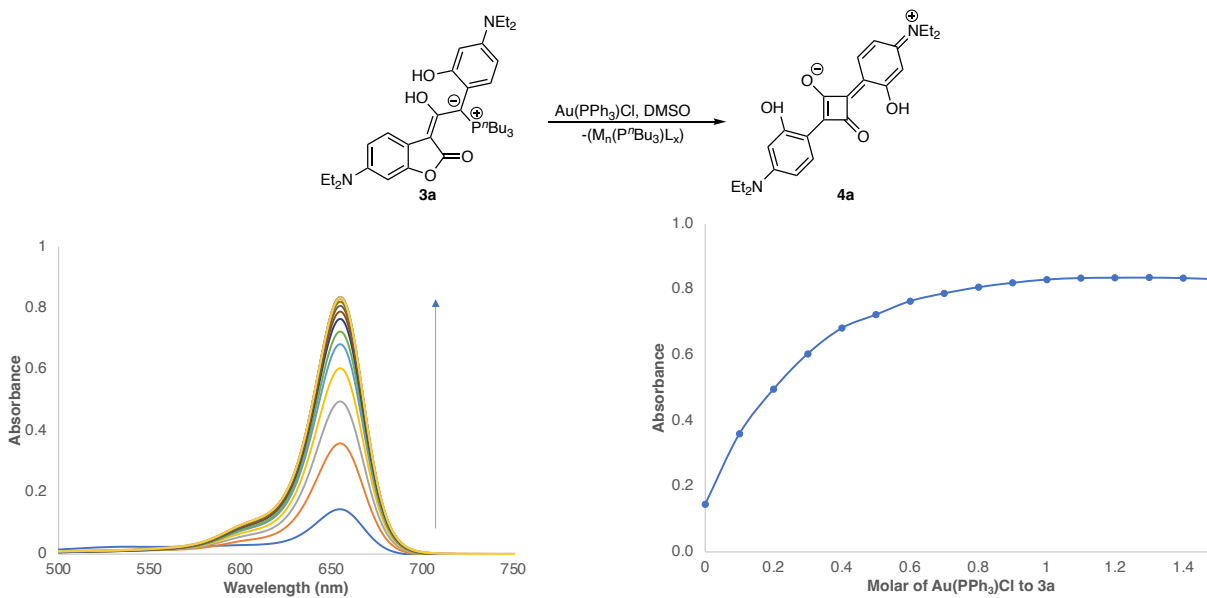


**Figure S4:** Titration of  $Au(PPh_3)Cl$  into a solution of benzofuranone ylide **3a** at 4.95  $\mu$ M in DMSO.



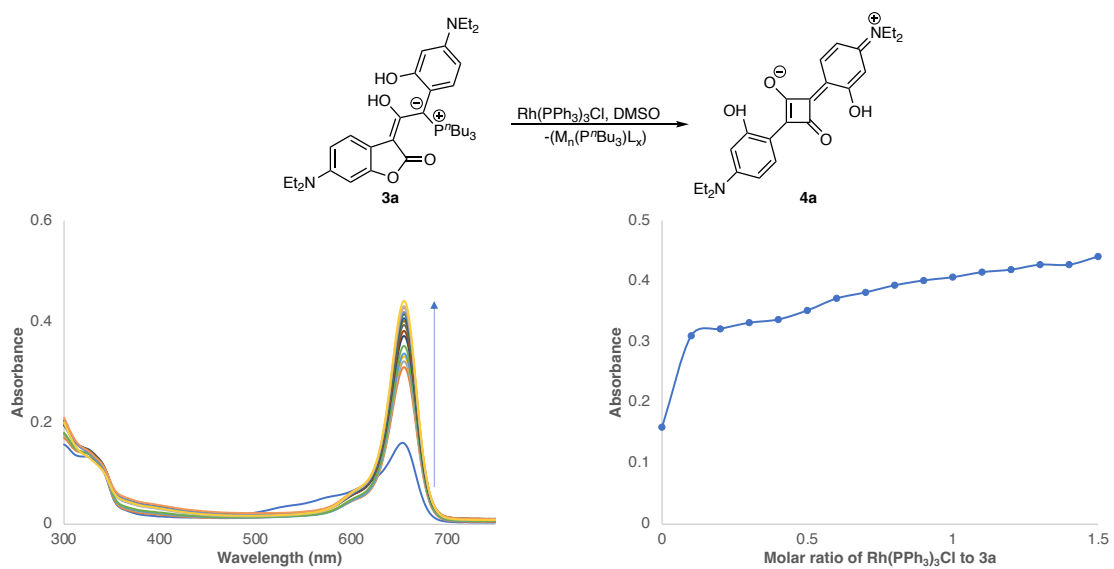


**Figure S5:** Titration of Rh(PPh<sub>3</sub>)<sub>3</sub>Cl into a solution of benzofuranone ylide **3a** at 4.96 μM in DMSO.

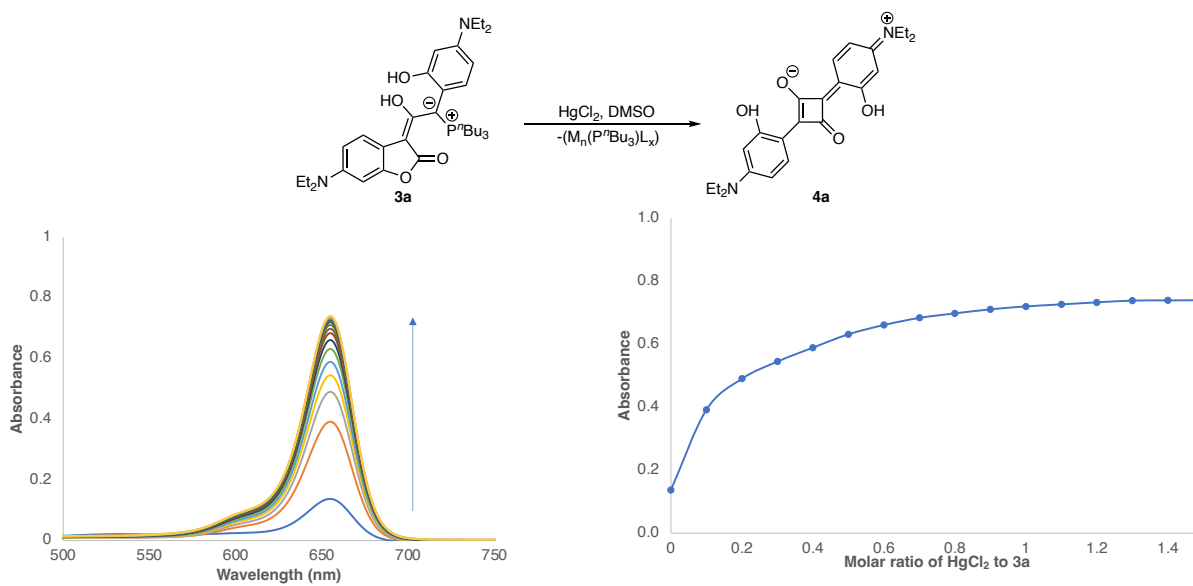


**Figure S6:** Titration of HgCl<sub>2</sub> into a solution of benzofuranone ylide **3a** at 4.95 μM in DMSO.

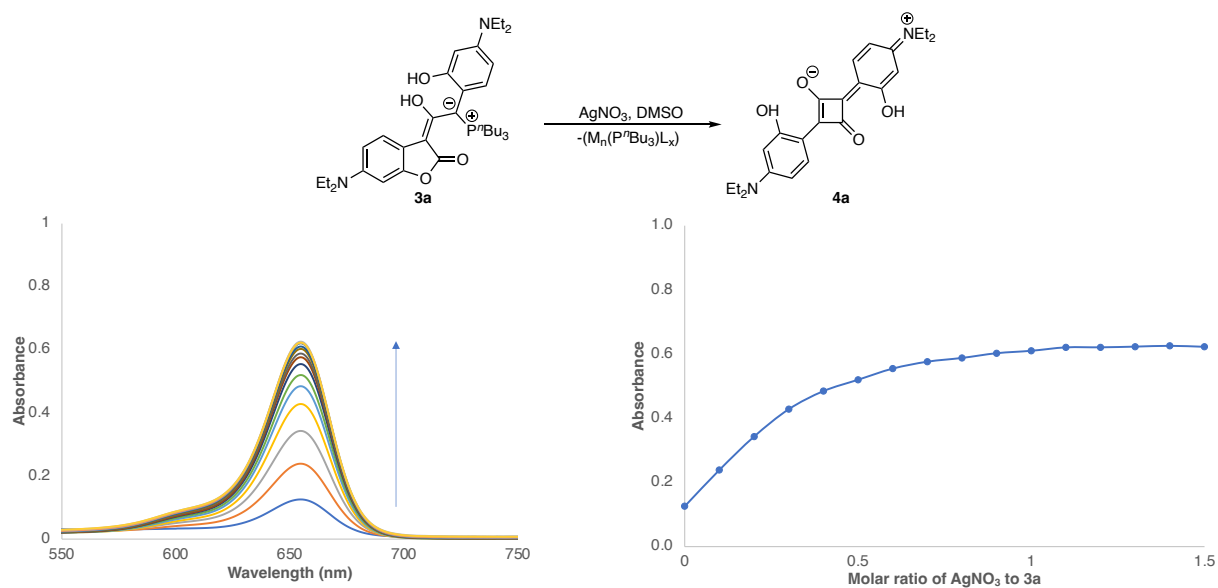


**Figure S7:** Titration of  $\text{AgNO}_3$  into a solution of benzofuranone ylide **3a** at  $4.96 \mu\text{M}$  in DMSO.

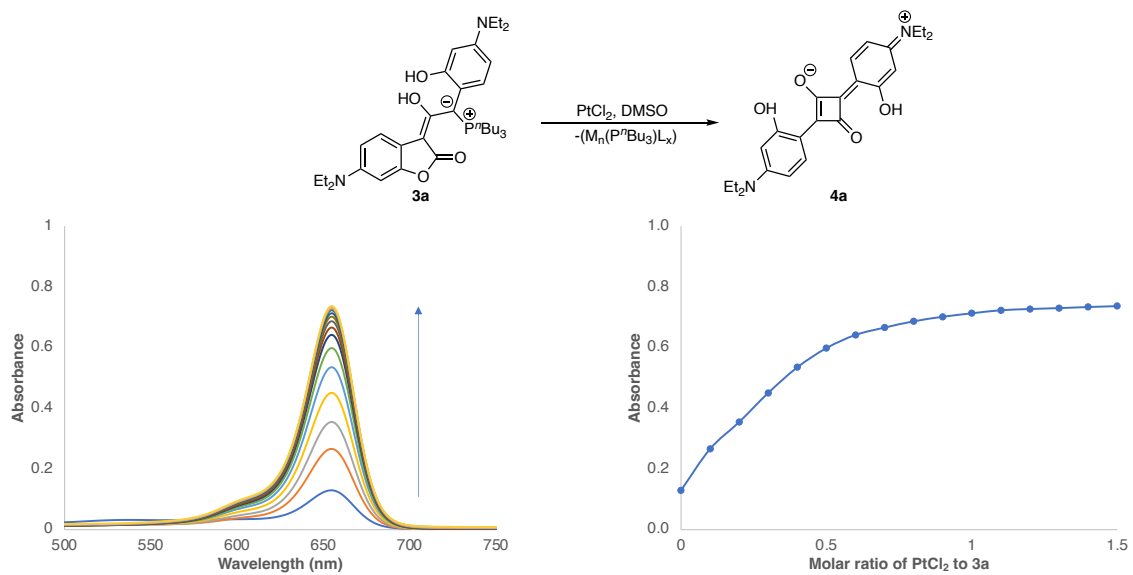


**Figure S8:** Titration of  $\text{PtCl}_2$  into a solution of benzofuranone ylide **3a** at  $4.96 \mu\text{M}$  in DMSO.

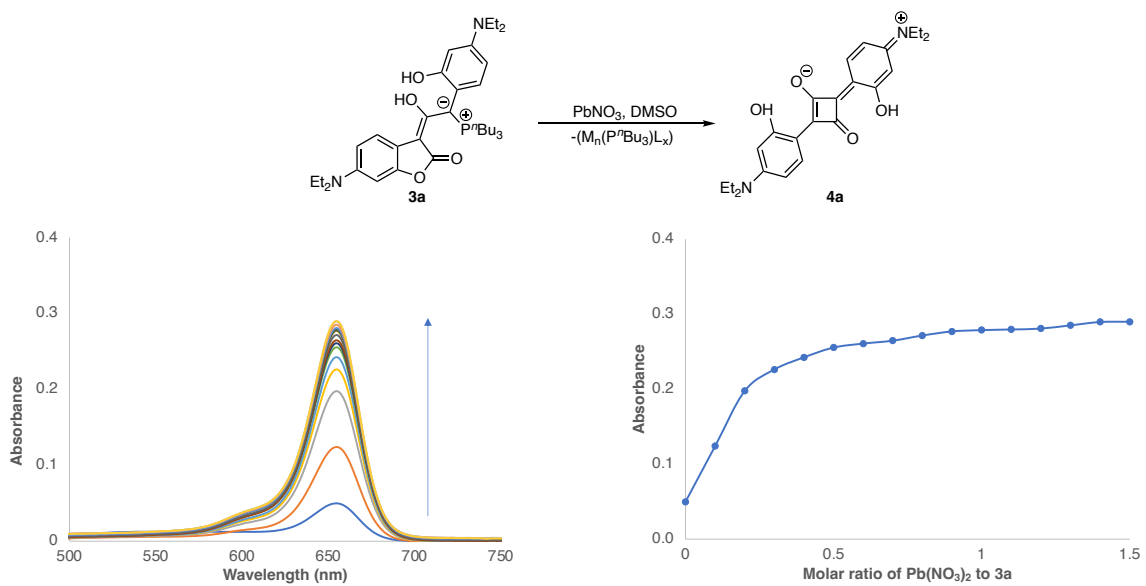


**Figure S9:** Titration of  $\text{Pb}(\text{NO}_3)_2$  into a solution of benzofuranone ylide **3a** at  $4.96 \mu\text{M}$  in DMSO.

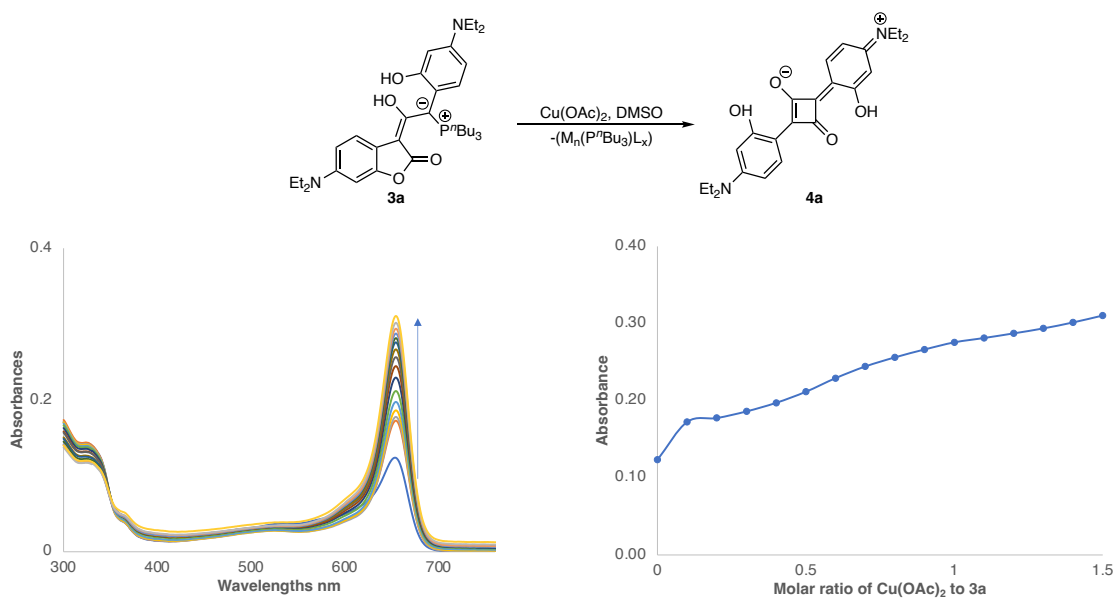


**Figure S10:** Titration of  $\text{Cu}(\text{OAc})_2$  into a solution of benzofuranone ylide **3a** at  $4.95 \mu\text{M}$  in DMSO.

### Beer's law analysis of SQ 4b in DMSO

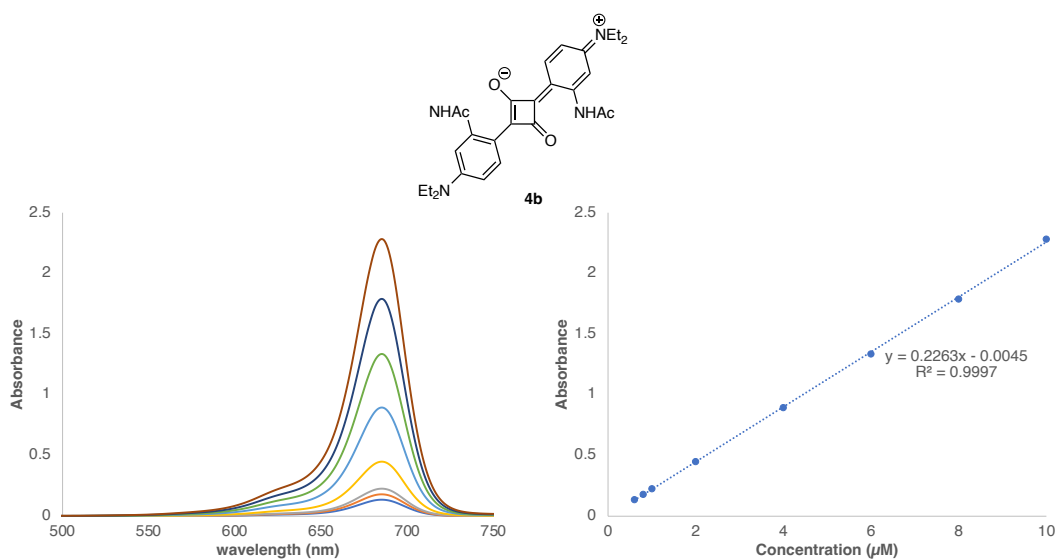


**Figure S11:** Beer's law analysis of squaraine of **SQ 4b** from 0.6 µM to 10 µM. Linearity is maintained as high as 2.28 absorbance units at 685 nm and an extinction coefficient of  $2.26 \times 10^7$  L mol<sup>-1</sup>cm<sup>-1</sup> was obtained.

UV-Vis spectral analysis of **4b** in DMSO is shown in **Figure S11**. Beer's law analysis shows a  $\lambda_{\text{max}}$  at 685 nm over the concentration range tested. Linear adherence to the Beer plot was maintained as high as 2.28 absorbance units. The molar extinction coefficient in DMSO was determined to be  $2.26 \times 10^7$  L mol<sup>-1</sup> cm<sup>-1</sup> from the slope of the absorbance/concentration plot at 685 nm for **4b**.

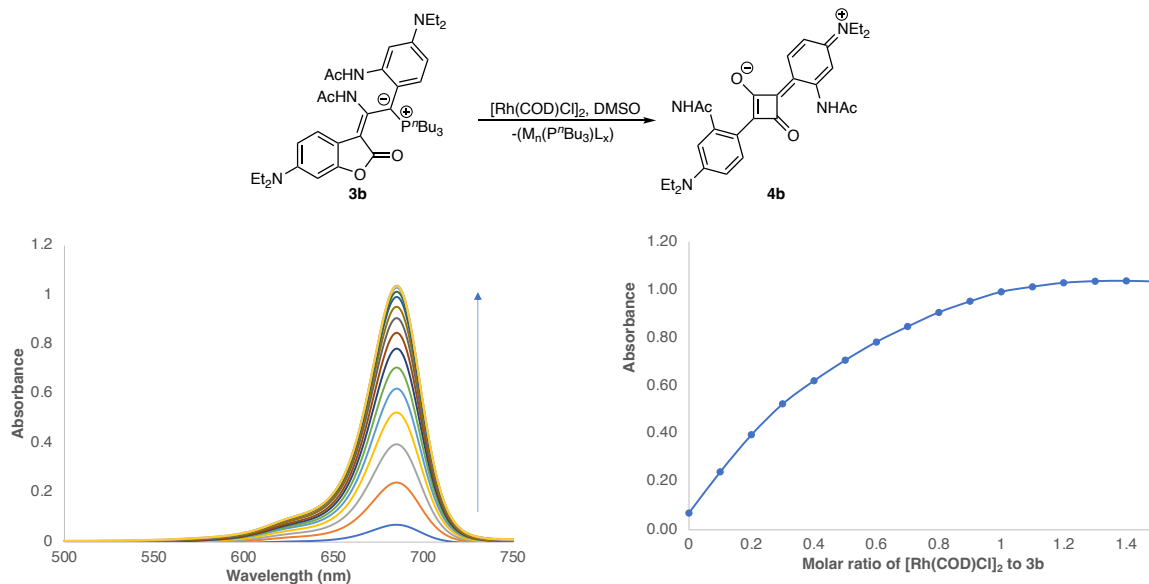


**Figure S12:** Titration of [Rh(COD)Cl]<sub>2</sub> into a solution of oxindole ylide **3b** at 5.03 µM in DMSO.

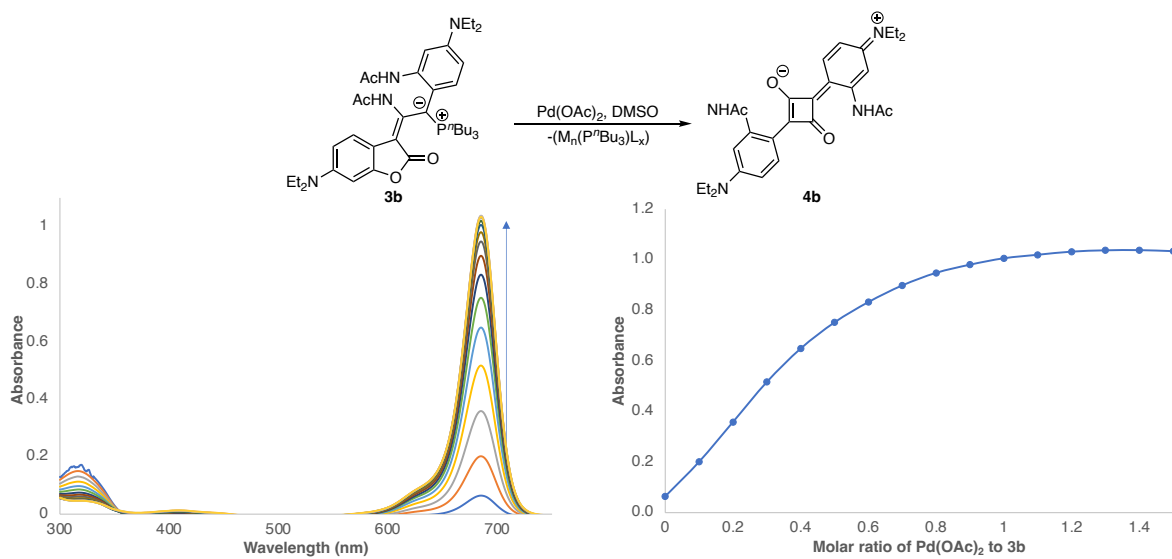


**Figure S13:** Titration of  $\text{Pd}(\text{OAc})_2$  into a solution of oxindole ylide **3b** at  $5.02 \mu\text{M}$  in DMSO.

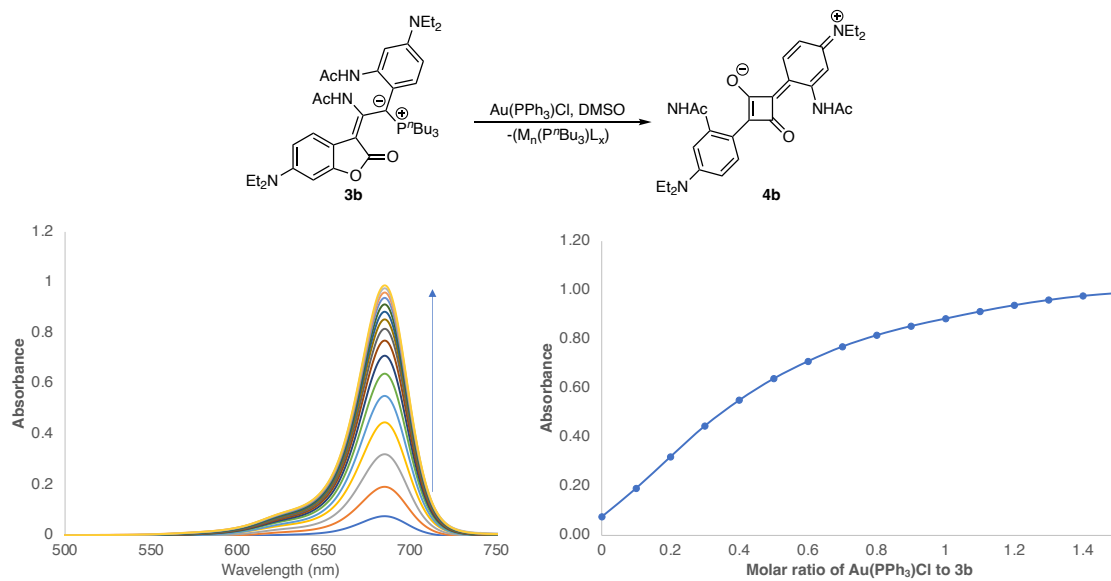


**Figure S14:** Titration of  $\text{Au}(\text{PPh}_3)\text{Cl}$  into a solution of oxindole ylide **3b** at  $5.03 \mu\text{M}$  in DMSO.

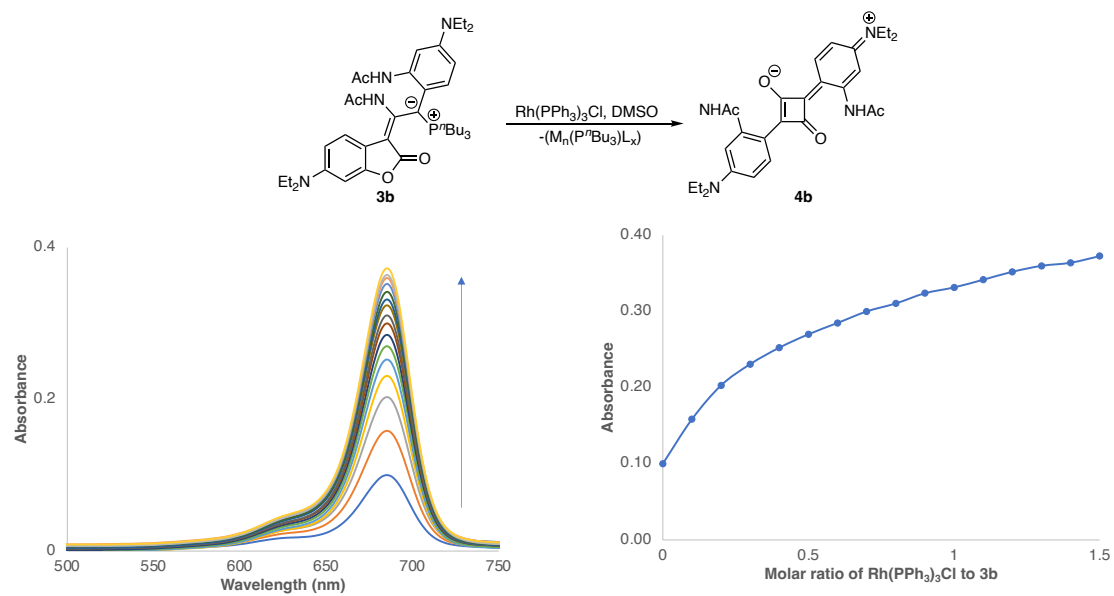


**Figure S15:** Titration of  $\text{Rh}(\text{PPh}_3)_3\text{Cl}$  into a solution of oxindole ylide **3b** at  $5.03 \mu\text{M}$  in DMSO.

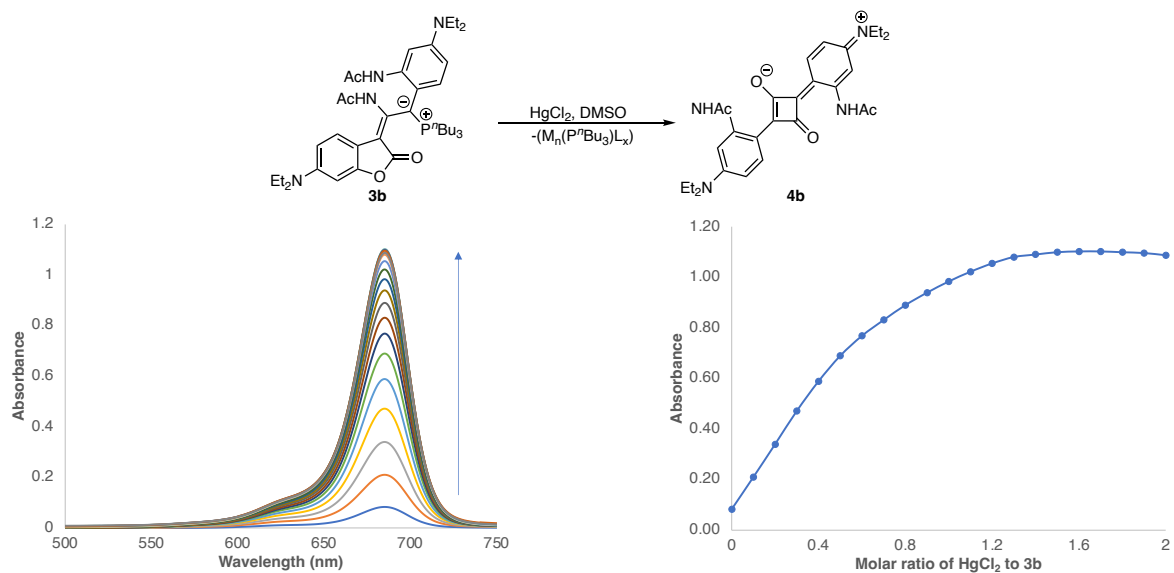


**Figure S16:** Titration of  $\text{HgCl}_2$  into a solution of oxindole ylide **3b** at  $5.03 \mu\text{M}$  in DMSO.

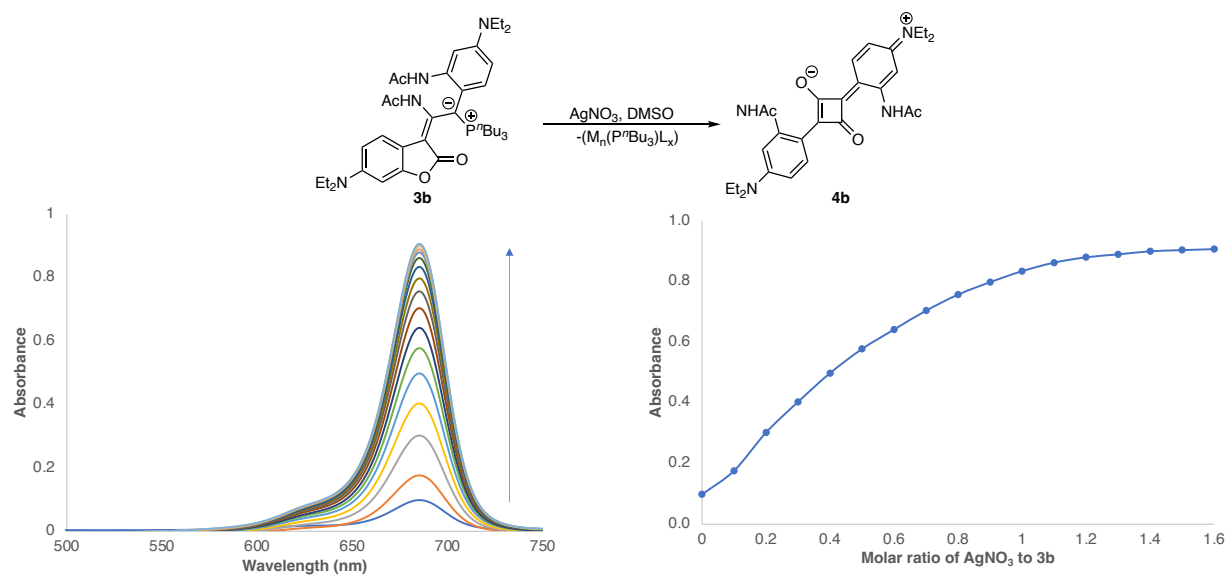


**Figure S17:** Titration of  $\text{AgNO}_3$  into a solution of oxindole ylide **3b** at  $5.00 \mu\text{M}$  in DMSO.

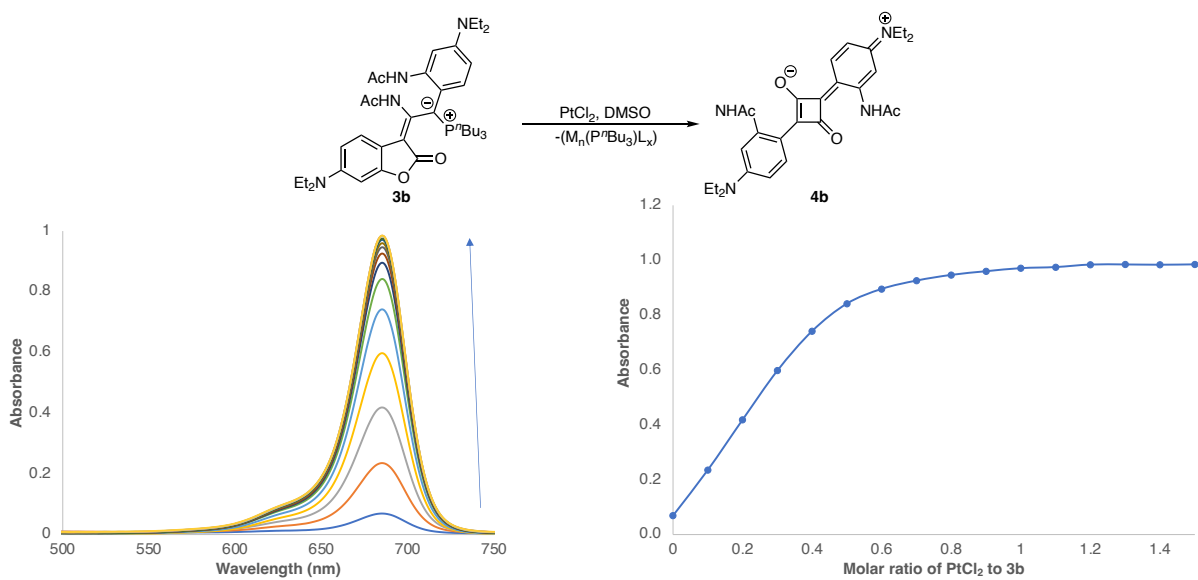


**Figure S18:** Titration of  $\text{PtCl}_2$  into a solution of oxindole ylide **3b** at  $5.00 \mu\text{M}$  in DMSO.

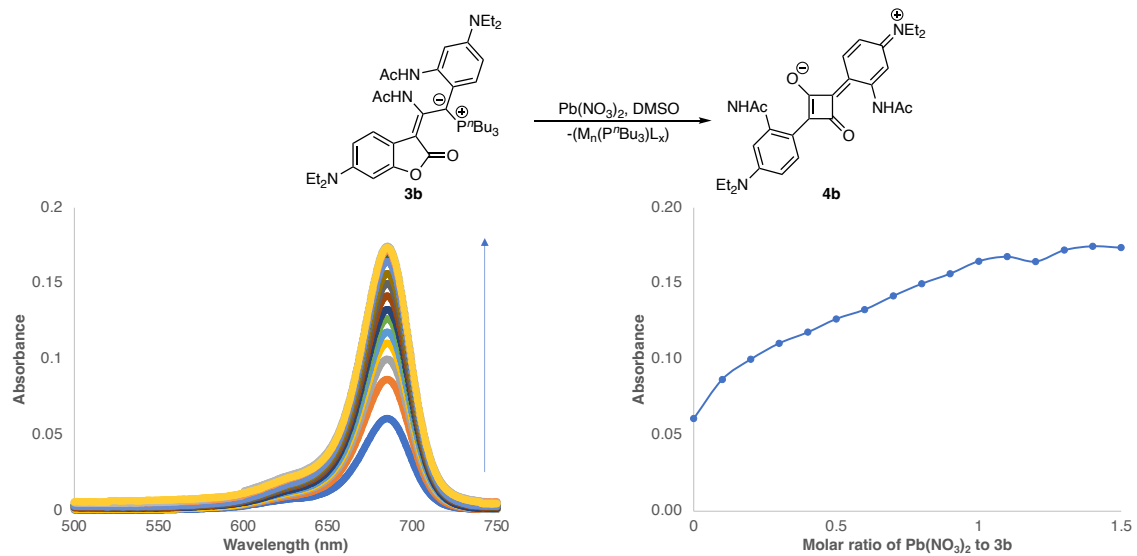


**Figure S19:** Titration of  $\text{Pb}(\text{NO}_3)_2$  into a solution of oxindole ylide **3b** at  $5.00 \mu\text{M}$  in DMSO.

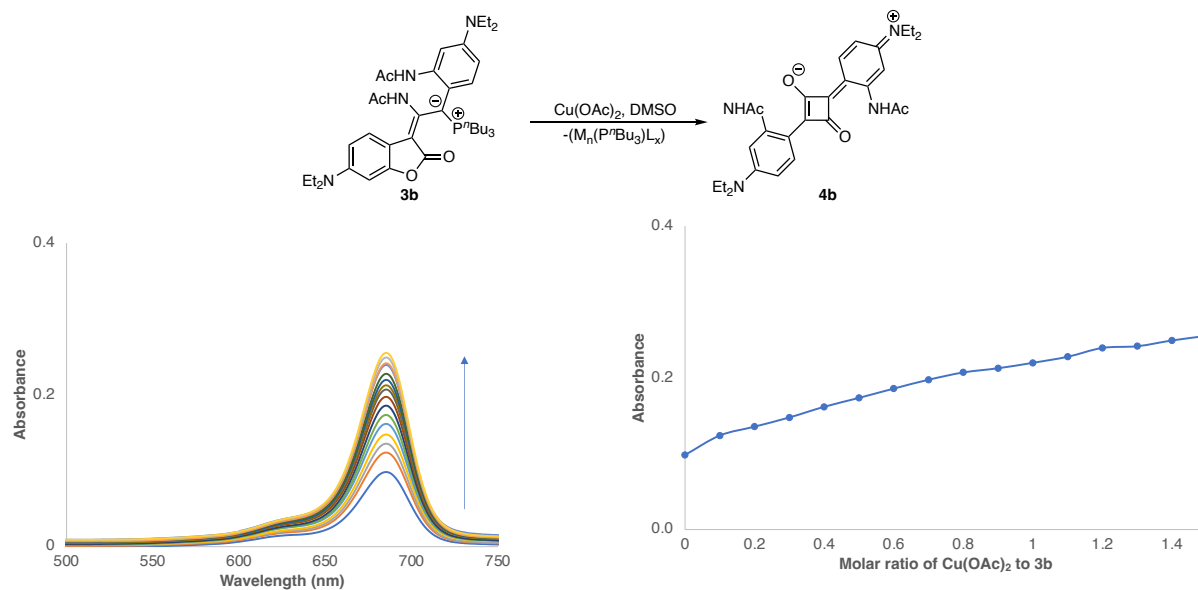


**Figure S20:** Titration of  $\text{Cu}(\text{OAc})_2$  into a solution of oxindole ylide **3b** at  $5.03 \mu\text{M}$  in DMSO.



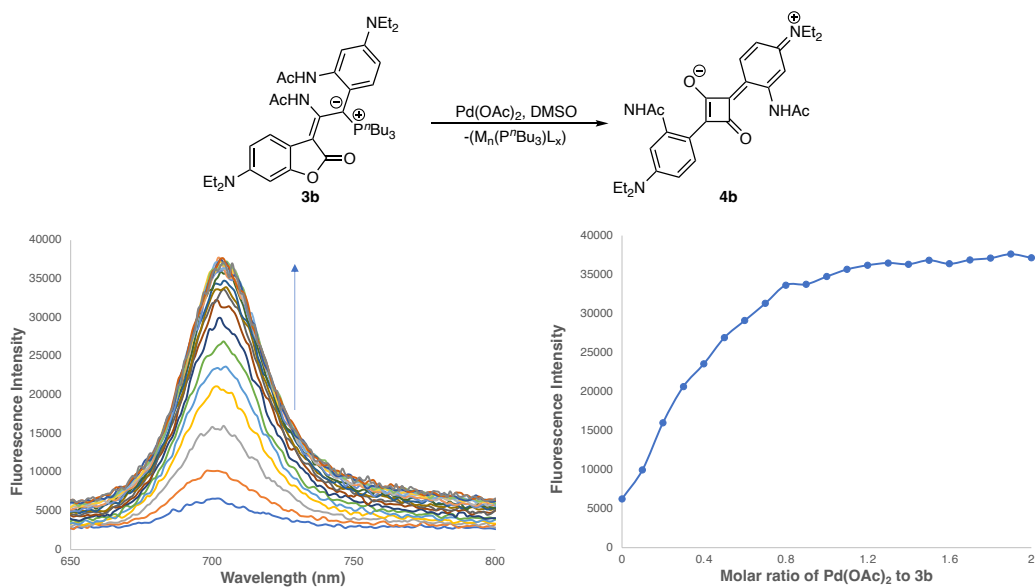


**Figure S21:** Changes in emission of ylide **3b** upon addition of  $\text{Pd}(\text{OAc})_2$  (0-2 eq.) in DMSO (5.00  $\mu\text{M}$ )

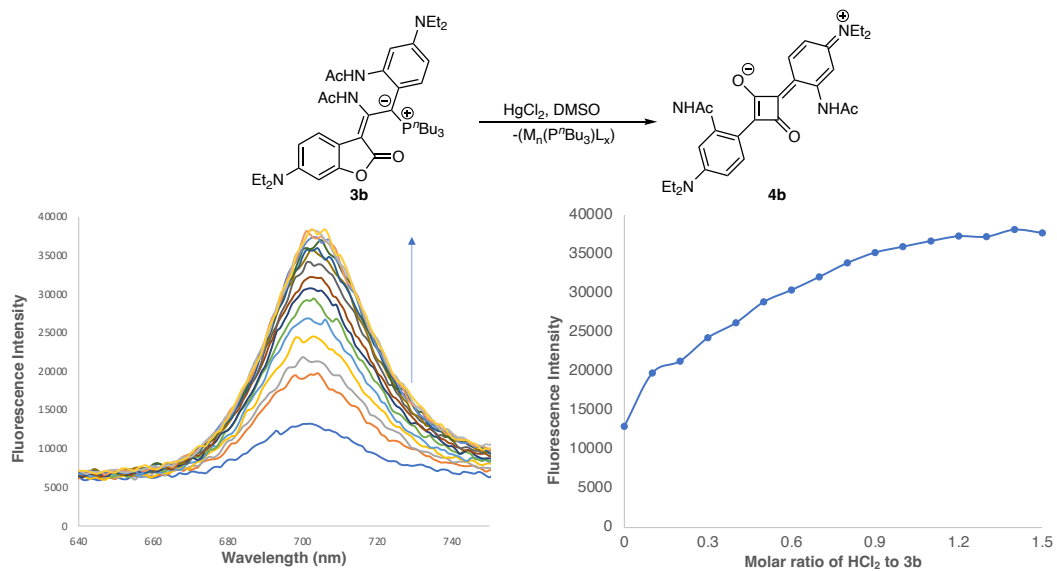


**Figure S22:** Changes in emission of ylide **3b** upon addition of  $\text{HgCl}_2$  (0-1.5 eq.) in DMSO (5.00  $\mu\text{M}$ )

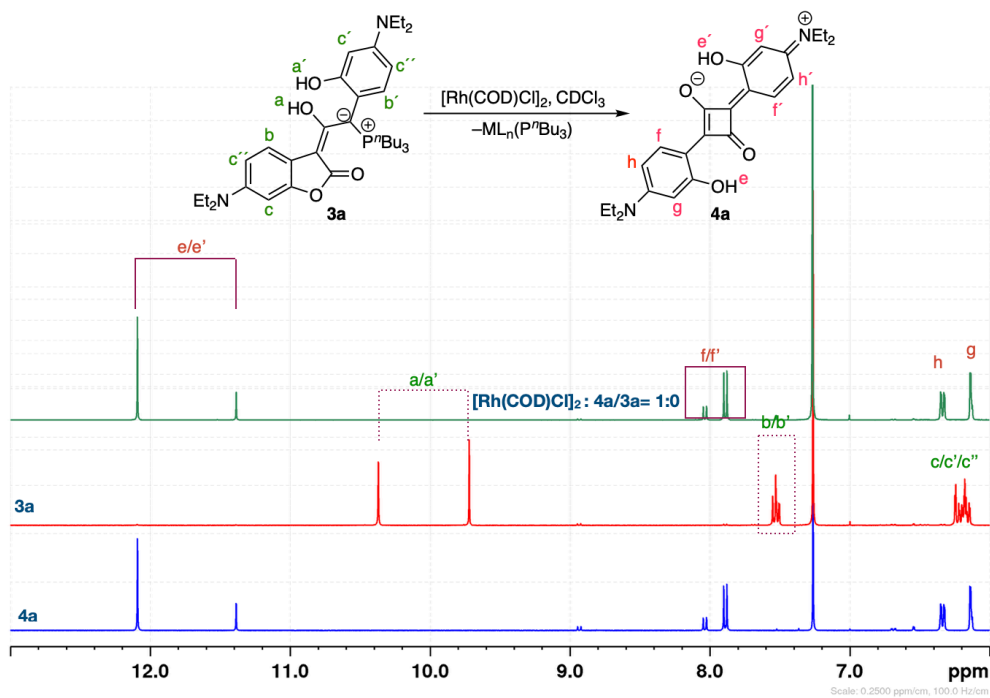


**Figure S23:** Partial  $^1\text{H}$  NMR spectra (500 MHz,  $\text{CDCl}_3$ ) that illustrates conversion of **3a** to **4a** upon addition of  $[\text{Rh}(\text{COD})\text{Cl}]_2$ . The ratio of **4a/3a** was determined by  $^1\text{H}$  NMR.

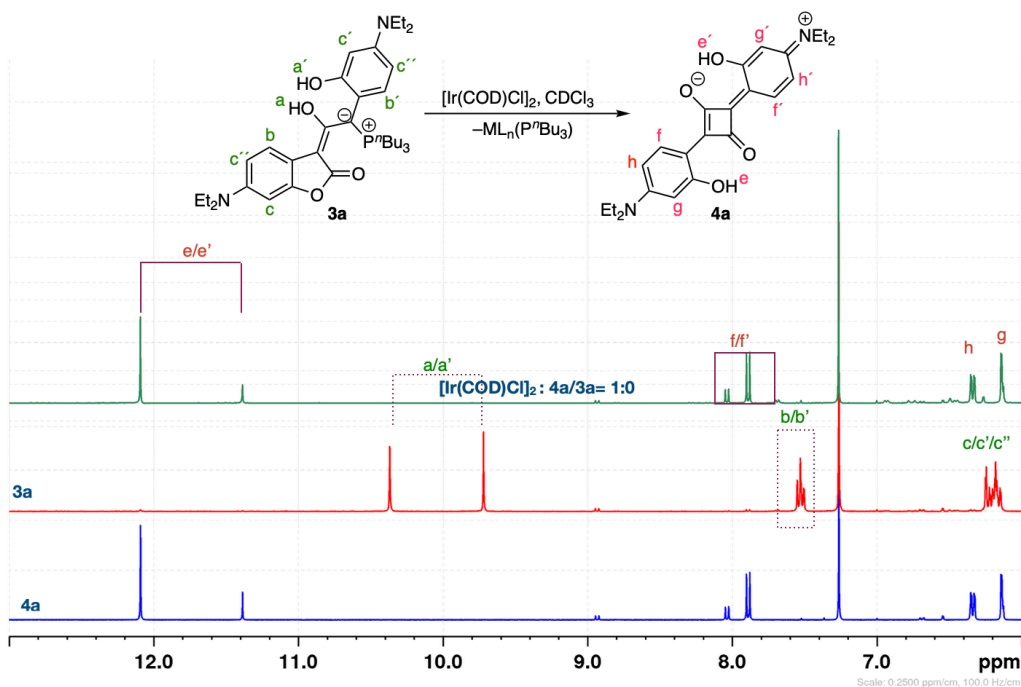


**Figure S23:** Partial  $^1\text{H}$  NMR spectra (500 MHz,  $\text{CDCl}_3$ ) that illustrates conversion of **3a** to **4a** upon addition of  $[\text{Ir}(\text{COD})\text{Cl}]_2$ . The ratio of **4a/3a** was determined by  $^1\text{H}$  NMR.

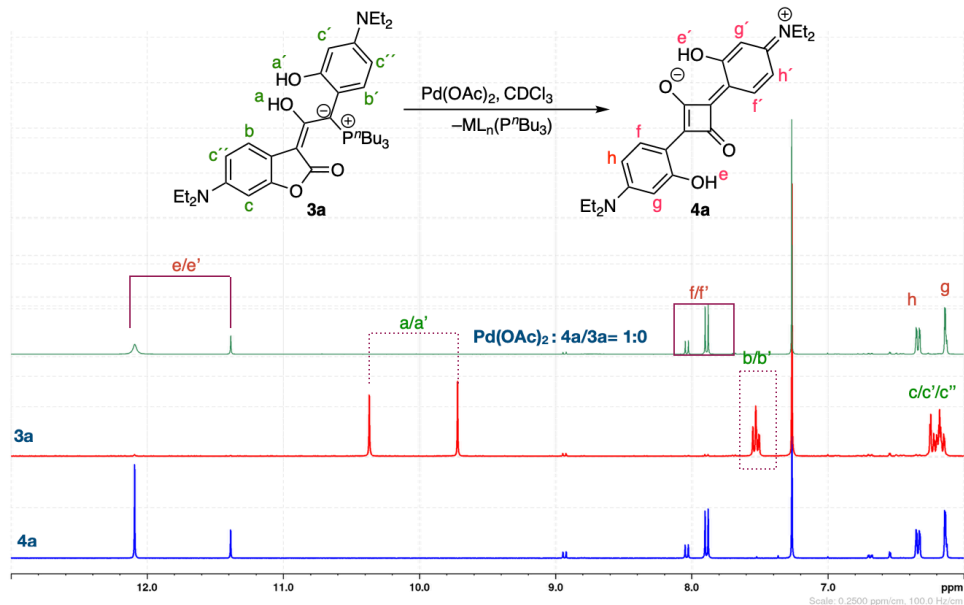


**Figure S25:** Partial  $^1\text{H}$  NMR spectra (500 MHz,  $\text{CDCl}_3$ ) that illustrates conversion of **3a** to **4a** upon addition of  $\text{Pd}(\text{OAc})_2$ . The ratio of **4a/3a** was determined by  $^1\text{H}$  NMR.

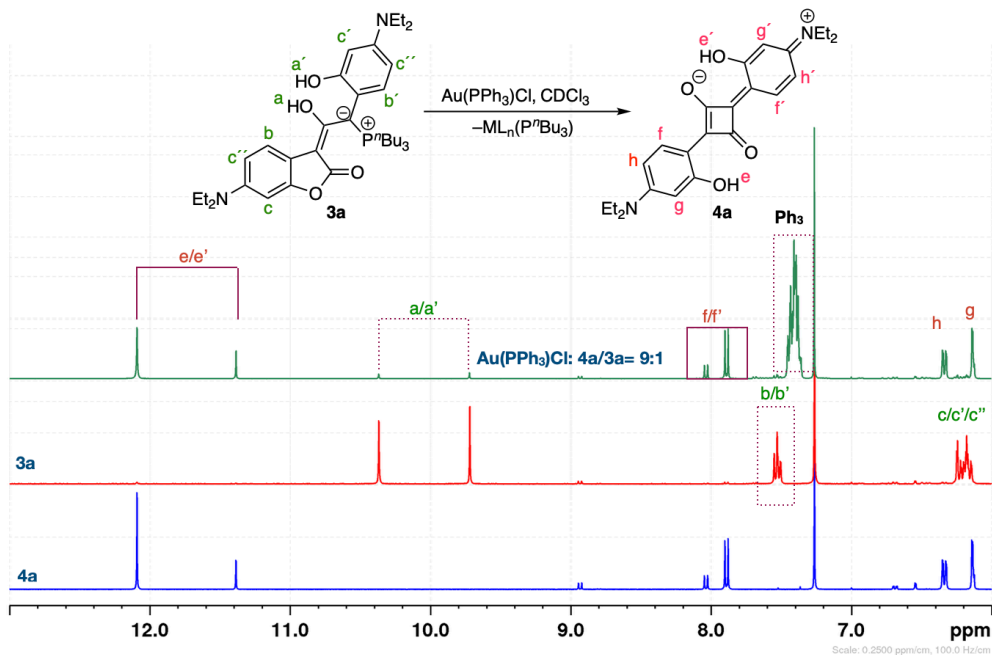


**Figure S26:** Partial  $^1\text{H}$  NMR spectra (500 MHz,  $\text{CDCl}_3$ ) that illustrates conversion of **3a** to **4a** upon addition of  $\text{Au}(\text{PPh}_3)\text{Cl}$ . The ratio of **4a/3a** was determined by  $^1\text{H}$  NMR.

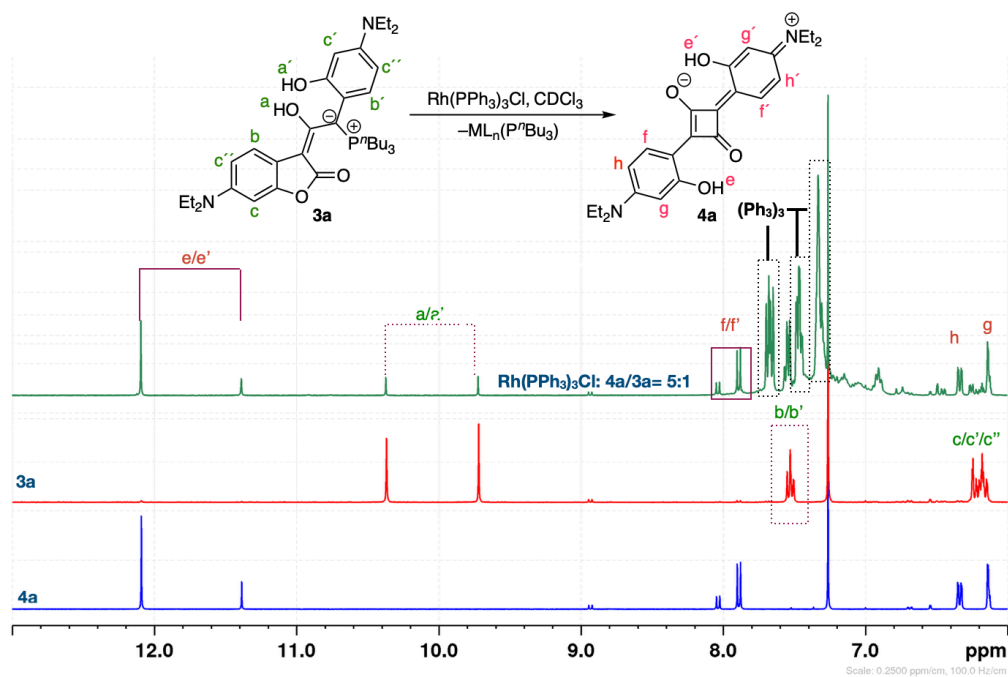


**Figure S27:** Partial  $^1\text{H}$  NMR spectra (500 MHz,  $\text{CDCl}_3$ ) that illustrates conversion of **3a** to **4a** upon addition of  $\text{Rh}(\text{PPh}_3)_3\text{Cl}$ . The ratio of **4a/3a** was determined by  $^1\text{H}$  NMR.

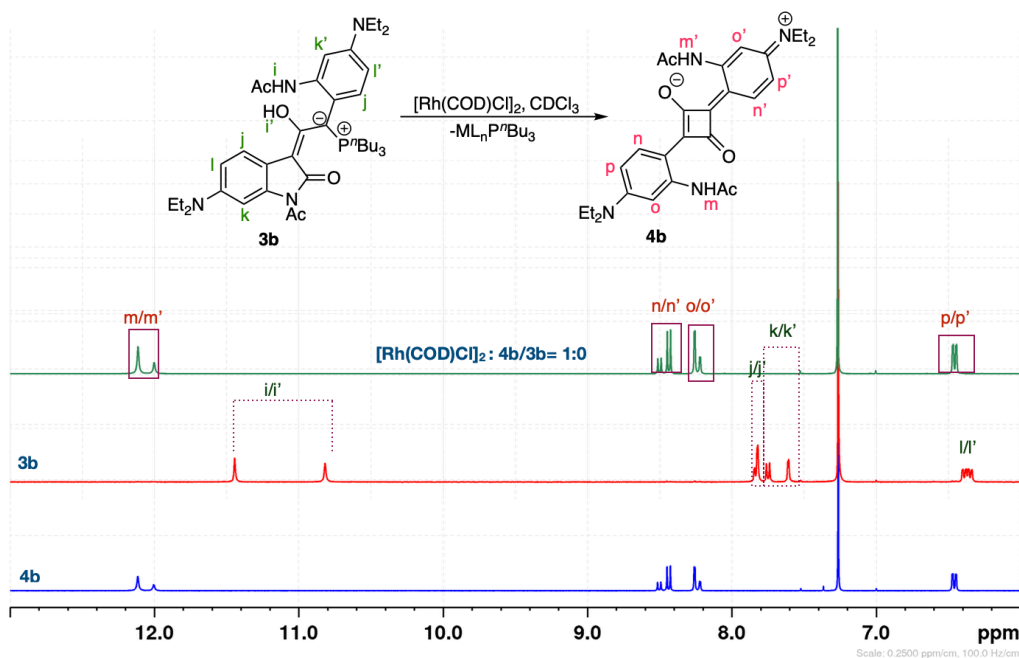


**Figure S28:** Partial  $^1\text{H}$  NMR spectra (500 MHz,  $\text{CDCl}_3$ ) that illustrates conversion of **3b** to **4b** upon addition of  $[\text{Rh}(\text{COD})\text{Cl}]_2$ . The ratio of **4b/3b** was determined by  $^1\text{H}$  NMR.

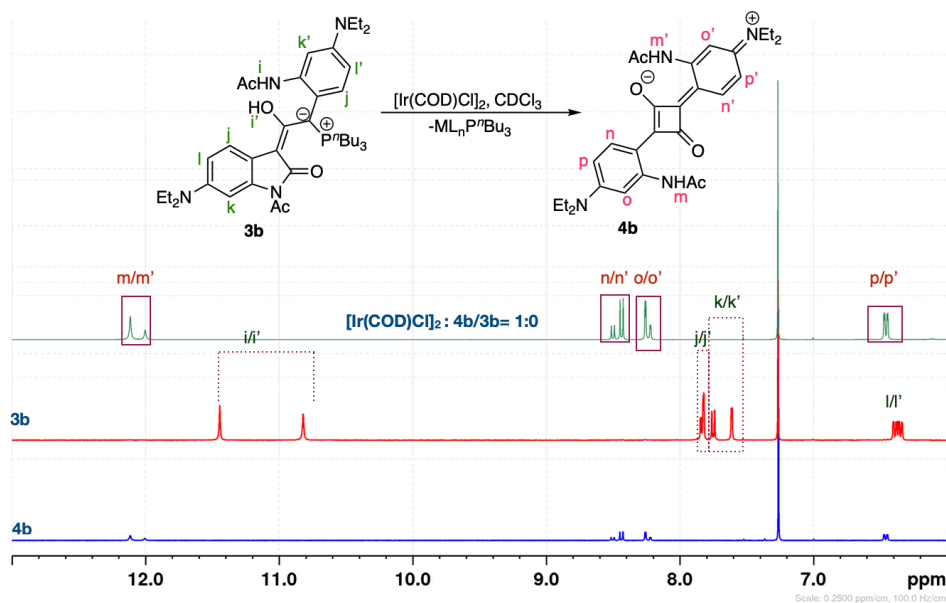


**Figure S29:** Partial  $^1\text{H}$  NMR spectra (500 MHz,  $\text{CDCl}_3$ ) that illustrates conversion of **3b** to **4b** upon addition of  $[\text{Ir}(\text{COD})\text{Cl}]_2$ . The ratio of **4b/3b** was determined by  $^1\text{H}$  NMR.

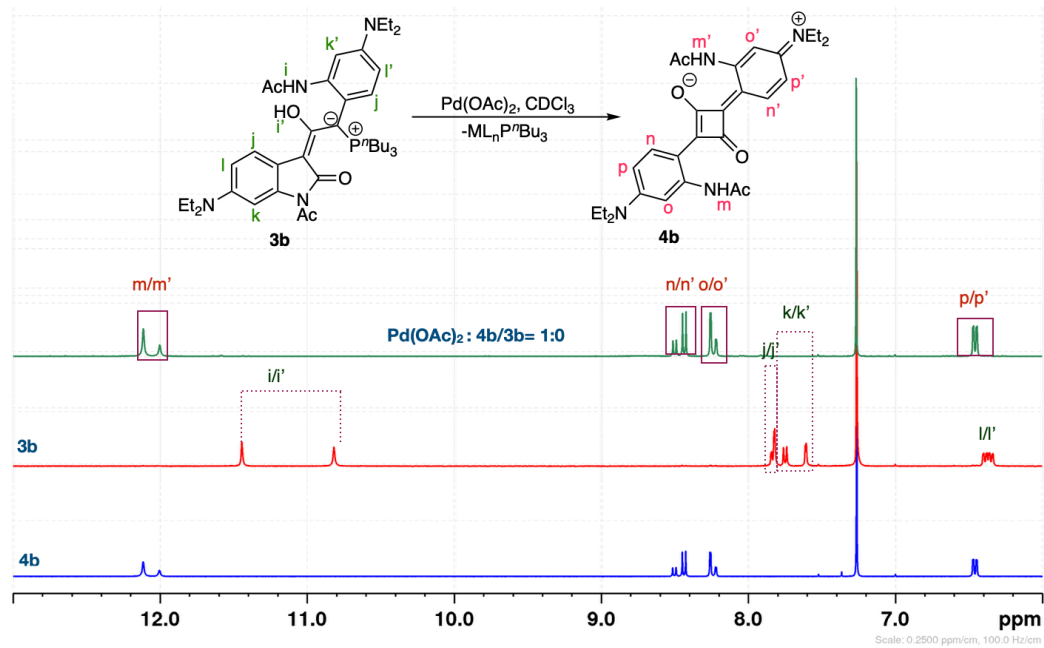


**Figure S30:** Partial  $^1\text{H}$  NMR spectra (500 MHz,  $\text{CDCl}_3$ ) that illustrates conversion of **3b** to **4b** upon addition of  $\text{Pd}(\text{OAc})_2$ . The ratio of **4b/3b** was determined by  $^1\text{H}$  NMR.

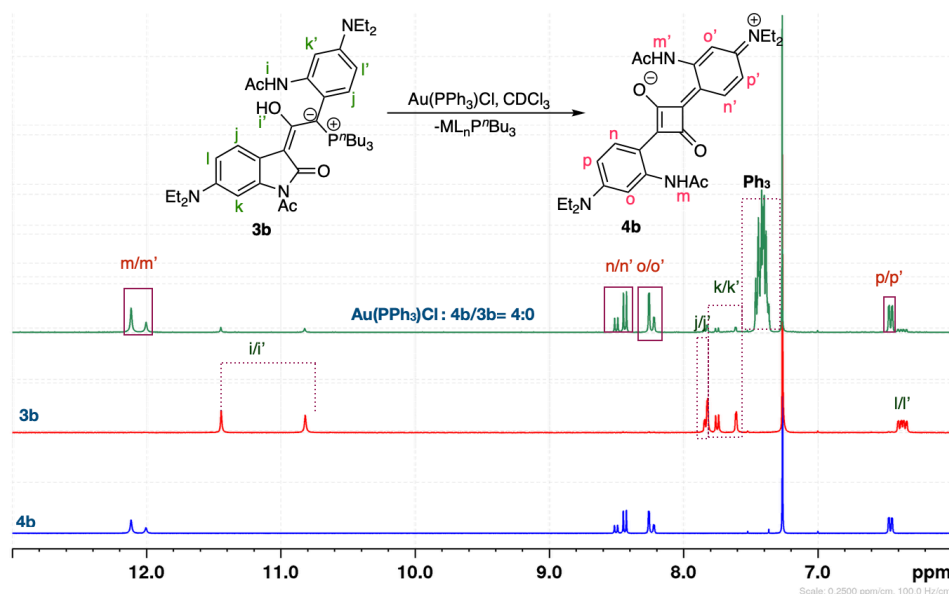


**Figure S31:** Partial  $^1\text{H}$  NMR spectra (500 MHz,  $\text{CDCl}_3$ ) that illustrates conversion of **3b** to **4b** upon addition of  $\text{Au}(\text{PPh}_3)\text{Cl}$ . The ratio of **4b/3b** was determined by  $^1\text{H}$  NMR.

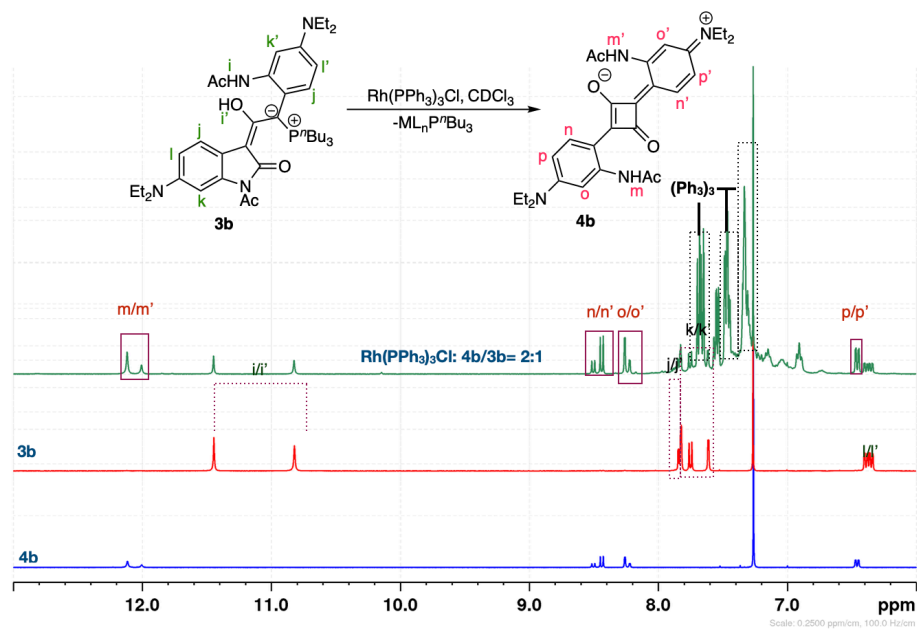


**Figure S32:** Partial  $^1\text{H}$  NMR spectra (500 MHz,  $\text{CDCl}_3$ ) that illustrates conversion of **3b** to **4b** upon addition of  $\text{Rh}(\text{PPh}_3)_3\text{Cl}$ . The ratio of **4b/3b** was determined by  $^1\text{H}$  NMR.

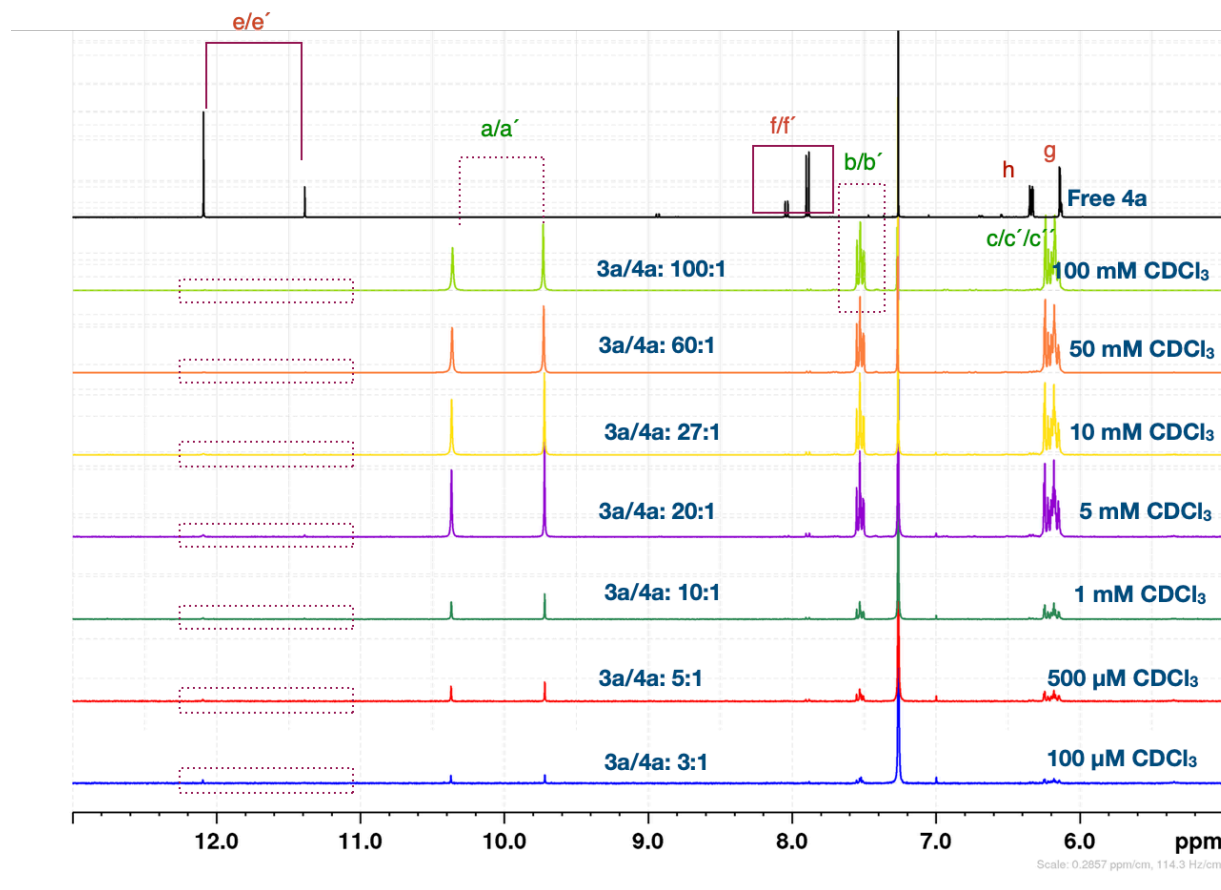
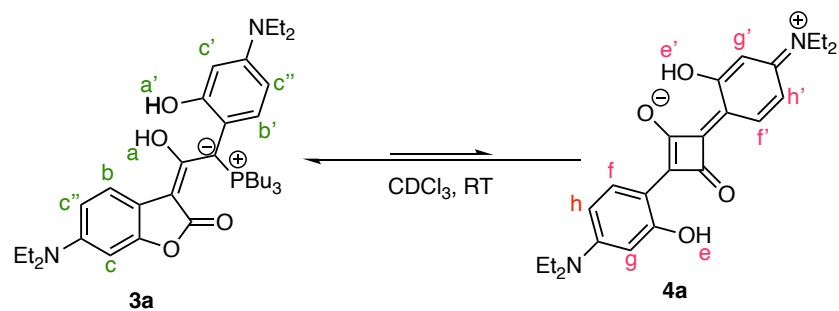


**Figure S33:** Partial  $^1\text{H}$  NMR spectra (500 MHz,  $\text{CDCl}_3$ ) that illustrates conversion of **3a** to **4a** with different concentration. The ratio of **3a/4a** was determined by  $^1\text{H}$  NMR **a/e** peaks integration.

## References

- (1) Bacher, E. P.; Koh, K. J.; Lepore, A. J.; Oliver, A. G.; Wiest, O.; Ashfeld, B. L. A Phosphine-Mediated Dearomative Skeletal Rearrangement of Dianiline Squaraine Dyes. *Org. Lett.* **2021**, *23* (8), 2853–2857.
- (2) Lepore, A. J.; Pena-Romero, D.; Smith, B. D.; Ashfeld, B. L. Nucleophilic Addition of Phosphorus(III) Derivatives to Squaraines: Colorimetric Detection of Transition Metal-Mediated or Thermal Reversion. *Chem. Commun.* **2019**, *55* (22), 3286–3289.